Fusion Engineering and Design 190 (2023) 113500

Contents lists available at ScienceDirect

Fusion Engineering and Design

journal homepage: www.elsevier.com/locate/fusengdes

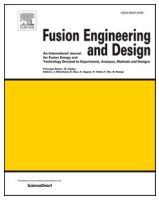

Voltages in the ITER magnets during operation

Salvatore Ventre [a], Guglielmo Rubinacci [b,*], Pierre Bauer [c], Gabriele Colombo [d]

[a] Dipartimento di Ingegneria Elettrica e dell'Informazione "Maurizio Scarano", Università degli Studi di Cassino e del Lazio Meridionale, CREATE, Via di Biasio n. 43, Cassino 03043, Italy
[b] Dipartimento di Ingegneria Elettrica e delle Tecnologie dell'Informazione, Università degli Studi di Napoli Federico II, CREATE, via Claudio n. 21, Napoli 80125, Italy
[c] Magnet Section, ITER Organization, Route de Vinon-sur-Verdon, CS 90 046, St. Paul Lez Durance 13067 CEDEX, France
[d] Alma Mater Studiorum, Università degli Studi di Bologna, Via Zamboni, 33, Bologna 40126, Italy

ARTICLE INFO

Keywords:
Superconducting magnet system
Quench protection
Induced voltages
Computational electromagnetism

ABSTRACT

Powerful electromagnetic transients characterize the operation of the ITER superconducting magnet system. This is especially the case for so-called plasma disruptions, but also during plasma current initiation and termination and during the fast discharge of the magnets for quench protection. To model these electromagnetic transients the CARIDDI code (Albanese and Rubinacci, 1988) has been used to calculate the induced voltages in several magnet quench detection loops during operational events of interest. The numerical model implemented in CARIDDI, based on an integral formulation discretized in terms of edge elements, is shown to be particularly well suited for analysing these transients which require a high level of precision. Note that, although we will mostly present results obtained with CARIDDI, all calculations were cross-checked with other codes and methods, most notably (ANSYS Maxwell, 2022).

1. Introduction

The calculation of the voltages occurring inside the coils and their supporting structures during the operational scenarios is an essential part of the electrical performance characterization of the ITER coils. The following discusses such calculations for a stand-alone CS Module (CSM) during an exponential discharge from 40 kA/turn (τ=6 s). This case is convenient for such study because it is relatively simple and experimental data are available from the recent factory testing.

The CS modules ([3], Fig. 1, Table 1) having a large inductance (order 1 H) and being ramped fast, the inductive voltages across their terminals can reach ~10 kV during operation. The voltages generated locally at the start of a quench of the superconductor (i.e. an accidental transition from the super- to the normal-conducting state) are of the order of several times 100 mV. Ideally the inductive voltages therefore need to be suppressed to the 10 mV level to allow unambiguous quench detection. A number of measures are implemented to bridge this detection gap. First, the coil is equipped with voltage taps at the level of Double Pancakes (DP), reducing the inductive voltages by a factor of 20 (the quench rarely spans many pancakes and if it did, it would be easy to detect). That reduces the needed inductive voltage rejection ratio, i.e. the ratio of inductive voltage and allowed residual inductive voltage, to 1000–10,000 (but increases the number of wires). This rejection ratio is possibly within reach for the Co-Wound-Tape (CWT) method. According to it the CS [2] conductors are wrapped with Co-Wound-Tapes (CWT), which allow to form a voltage tap system with minimal inductive pick-up (Fig. 2). A voltage measurement then consists of subtracting the CWT voltage over the DP from the DP voltage, which removes a large fraction of the inductive voltage (see Fig. 2). This difference voltage is referred to as the compensated voltage. Other techniques such a subtracting the voltages of similar DP can also be performed (also on top of the CWT method for further refinement).

As will be shown in the following, the simulation of the compensated voltages between the voltage taps and CWT during a scenario (here a fast discharge) is not trivial. First and foremost a precision of 10^{-4} (or even a few times 10^{-5}) needs to be achieved by the calculation, which is a challenge, also given the size and complexity of the ITER coil system (and the models describing it).

The magnetic field topology of the CSM in the stand-alone configuration is close to that produced by a number of axisymmetric coaxial coils. The idealized version of the coil is therefore implemented in an axisymmetric model (a collection of 560 flat rings) with a perfectly axisymmetric (around the z-axis) current distribution and is therefore a purely 2D model. Note, however, that the twisting of the strands inside

* Corresponding author.
E-mail address: rubinacci@unina.it (G. Rubinacci).

https://doi.org/10.1016/j.fusengdes.2023.113500
Received 25 October 2022; Received in revised form 31 December 2022; Accepted 13 January 2023

Fig. 1. Top left – CS module 1 during assembly into the test facility at GA/USA, top right: CS module dummy winding trial, bottom left: cross-section of the CS conductor, bottom right: CWT assembly over the conductor insulation.

Table 1
CS Module main parameters.

Parameter	Value
Inner radius	1323 mm
Outer radius	2079.5 mm
Height	2147.3 mm
Number of pancakes	40
Number of turns per pancake	14
Total number of turns	556
Maximum current capability	25.02 MA (12.4 T)
Mass	111 310 kg

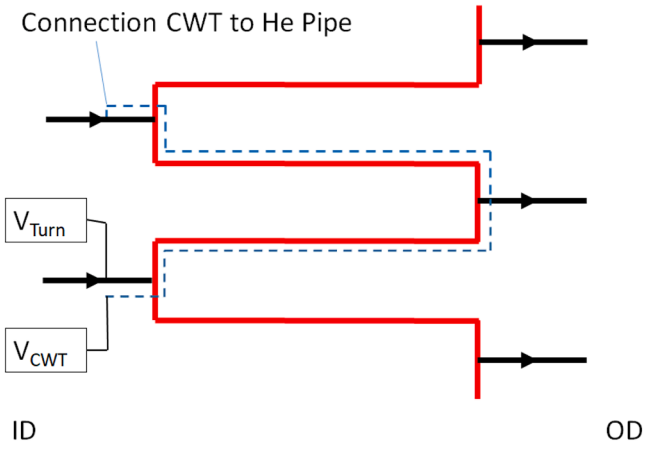

Fig. 2. Quench voltage measurement scheme in the CS (from Magnet Instrumentation DDD-9).

the cable generates a possible additional field perturbation that is parallel to the conductor axis (azimuthal) and the calculation of this effect requires a 3D model that has been also implemented and described in the paper.

In particular, these two models were implemented and applied for the calculations presented here: the "A-method", in which the inducing field is purely axisymmetric and the "E-method" or "Electrode-method" which requires a full 3-D description of the cable. They are both enabled by the CARIDDI code. The simpler A-method consists of calculating the voltage over the turn or CWT by integrating the vector-potential *A* over a line following the turn or the CWT. It is best applied when the CWT and/or the turn can be represented by a line (or thin wire). The electrode-method implements the actual shape of the conductor or the CWT and is therefore more elaborate and generally requires more computing resources and pre- and post-processing efforts. Although both methods are in principle applicable to 2D and 3D, CARIDDI (and Maxwell) implements the A-method only for 2D cases, while the E-method allows both 2D and 3D model calculations

The following discussion will introduce the mathematical and

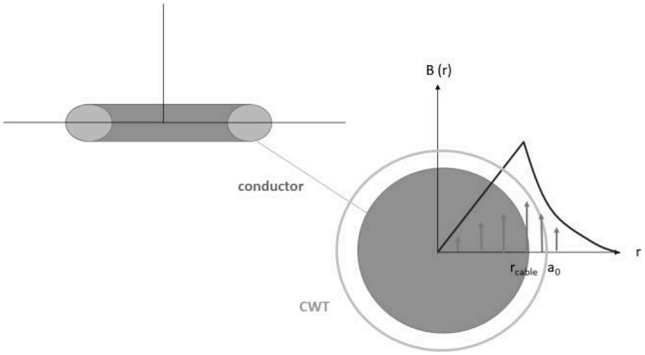

Fig. 3. Illustration for the self-field effect – cross-sectional view.

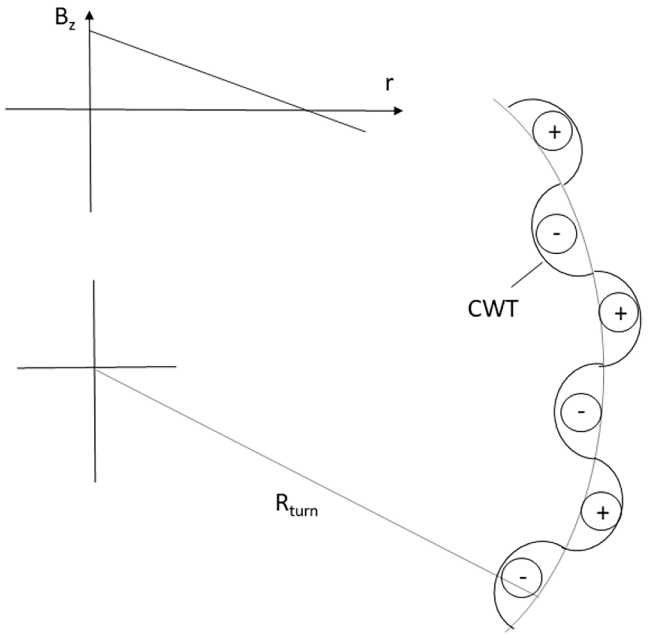

Fig. 4. Illustration for the field gradient effect – view from above (example of an inner turn).

modeling concepts, then present results for the CWT and turn voltages discussing single-turn models and multi-turn models.

2. Analytical model

As a first approximation a 1D analytical model [4] can be developed to describe the residual inductive voltages in a Co-Wound-Tape (CWT) system as introduced above. The compensated voltage is defined as the difference between the turn and CWT voltages: $V_{comp}= V_{turn} - V_{cwt}$. The model is limited to the 2D case, i.e. with only axisymmetric current sources. In this frame there are two important effects which need to be considered. These are the so-called "self-field-"and the "field gradient-" effects, where the self-field effect (Fig. 3) is dominating. The self-field effect originates from the conductor and the CWT integrating a different amount of flux related to the conductor self-field, which gives an imbalance between the turn and the CWT voltages.

The difference in compensated voltage per unit length is:

$$\Delta v_{comp} = \frac{\mu_0 j}{2\pi}\left(ln\frac{a_0}{r_{cable}}\right) \qquad \left[\frac{V}{m}\right] \tag{1}$$

where $a_0 > r_{cable}$ (a_0 the CWT radius, and r_{cable} the conductor radius). Based on this the residual compensated voltage between CWT and turn voltage in the CSM ($a_0 = 0.025$ m, $r_{cable} = 0.016$ m) is −0.6 mV/m for 6.66 kA/s (0.05 s into a fast discharge from 40 kA) per m of turn which gives −7.6 mV/turn for an outer CS turn and −5 mV/turn for an inner CS turn. The field gradient effect (Fig. 4) is essentially due to the field generated by all the other turns. If the externally applied field (the field generated by the other turns) is homogeneous over the conductor the effect disappears. But when there is a gradient, the CWT loses (or gains) flux at the inside, which is not equilibrated by the gain (or loss) of flux while it winds around the outside of the conductor (whether it is loss or gain depends on the sign of the field gradient). The conductor does not experience this effect, it only appears for the CWT.

The field gradient contribution to the compensated voltage Δv_{comp} can be estimated from the CWT radius a_0, and the time derivative of the spatial field gradient (d/dt d/drB_z):

$$\Delta v_{comp} = -\left(\frac{d}{dt}\frac{d}{dr}B_z\right)\frac{\pi a_0^2}{8} \qquad \left[\frac{V}{m}\right] \tag{2}$$

Table 2
Comparison of A_ϕ (Vs/m) inside the CSM @ 40 kA/turn calculated w. CARIDDI. *in CARIDDI the average A is calculated from the magnetic energy inside the turn conductor volume, ** calculated by sub-division of the turn into 292 filaments.

Turn	thick cond (center**)	thick cond (average*)	thick cond w. hole (center**)	thick cond w. hole (average*)
1	3.731523	3.729736	3.730867	3.7294673
294	5.410514	5.408726	5.409857	5.4084573

For a_0=0.025 m, $d/dtd/drB_z$ =8T/m/6 s the voltage calculated with the above is −0.33 mV/m (or 4.3 mV/2.8 mV) on a single outer/inner CS turn. Note that for the stand-alone CSM discharge the gradient effect has the same sign as the self-field effect, so it increases the compensated voltage. The effect expected from the gradient of the radial field is not considered here as it is smaller (but it is not negligible). Also note that this effect is independent of the CWT twist pitch, as long as the number of twist pitches over a turn is an integer.

So after addition of the gradient field effect the expected compensated voltage for the inner conductor is −11.9 mV for an outer turn and −7.8 mV/turn for an inner turn, as they have different length. Note again also that these numbers only apply to the case of the CWT going around one turn with an integer number of pitches. Integrating the turn lengths for a DP the expected compensated voltage becomes −276 mV. 3D effects are not described by this model, so it can only be compared to 2D model results.

3. Calculations of the vector-potential in the axisymmetric approximation

The azimuthally directed 2D vector-potential A_ϕ generated at the point $P(x_0, y_0, z_0)$ by n axisymmetric filamentary current sources lying flat in the x/y plane with current I_n and radius a_n is[1]:

$$A_\varphi(x_0,y_0,z_0) = \frac{\mu_0}{4\pi}\sum_{all\ sources\ n} I_n \oint \frac{r_n d\varphi}{\sqrt{(x_n(\varphi)-x_0)^2+(y_n(\varphi)-y_0)^2+(z_n(\varphi)-z_0)^2}}$$
$$= \frac{\mu_0}{\pi}\sum_{all\ sources\ n}\frac{I_n}{k_n}\sqrt{\frac{a_n}{\rho_0}}\left[\left(1-\frac{k_n^2}{2}\right)K(k_n)-E(k_n)\right]\left(\frac{Vs}{m}\right) \tag{3}$$

where $\rho_0 = \sqrt{x_0^2+y_0^2}$, $k_n = \sqrt{\frac{4\rho_0 a_n}{(\rho_0+a_n)^2+(z_0-z_n)^2}}$ and K and E are the complete elliptic integrals of the first and second kind defined for $0 < k < 1$ by

$$K(k) = \int_0^{\frac{\pi}{2}} \frac{d\theta}{\sqrt{1-k^2\sin^2\theta}}$$

and

$$E(k) = \int_0^{\frac{\pi}{2}} \sqrt{1-k^2\sin^2\theta}\, d\theta$$

The computation of the voltage for thick conductors requires a further step, in order to be consistent with the definition of the energy stored in them. Therefore, we expressed the voltage as $V = L\frac{dI}{dt}$, L being the inductance of the massive conductor defined as $L = 2\pi \iint_S \rho A_\varphi J_\varphi dS/I^2$. The surface takes into account the presence of the cooling channel in the middle of the conductor that needs to be excluded. Note, as shown in [5], that the vector potential needs to be

[1] Note the singularity when $(x,y,z)=(x_0,y_0,z_0)$. In this approach the singularity has been removed by computing the self contribution in the very high aspect ratio limit.

calculated with a precision to the fourth digit included (10^{-4}).

Table 2 gives the vector potential calculated with CARIDDI for the thick conductor case with and without hole, averaged over the conductor and in the center for turn 1 (an outer turn) and turn 294 (an inner turn) of the CSM. The vector-potential sampled in the center of the conductor is not relevant for the following and it is given only for reference purposes. The calculation of A in a specific point (for example in the center) is not performed automatically in CARIDDI and it is required to break down the respective conductor into a number of filaments to obtain an accurate value for A in this case (a minimum of 200 filaments is required, here 292 is used). Note the significant difference of the values in the table.

In the following section the turn-voltages calculated from the average vector potential and using a full implementation of the conductor geometry including the cooling hole (as for the calculation of the data for the last column in Table 2) will be discussed. On the other hand, the CWT (physically a fine wire) can be considered as a "line", and the vector-potential can be computed in the points forming this line, with no need of averaging.

Summarizing it is important to repeat that the actual geometry of the conductor in the model (diameter, cooling hole,..etc.) is critical for the precision. In some cases this needs to be implemented manually e.g. defining multiple (>200) current filaments.

4. Calculations of the voltage with the A-method

For flat current rings in the x/y plane the 2D turn voltage can be derived from the vector potential with:

$$U = \oint \frac{\partial \vec{A}}{\partial t} \cdot \vec{ds} = \frac{dA_{\varphi,turn}}{dt} 2\pi r_{turn} \ (V) \tag{4}$$

where in this case the component of the vector potential parallel to the turn path is A_ϕ (toroidal) and $2\pi r_{turn}$ the length of the turn. Since the magnetic field is perfectly axisymmetric in this case, one value of the vector potential per turn suffices (A doesn't vary along the turn). Note that, as discussed above, A_ϕ here is the average over the thick turn (also taking into account the presence of the cooling hole). Given the high levels of accuracy required, care has to be applied also for the time differentiation of the vector-potential. A central difference method or better is the minimum requirement.

4.1. Co-wound-tape voltages with the A-method (2D)

A number of aspects of the calculation of the CWT voltages were investigated with the A-method for a single turn model. These effects are:

- the minimum number of points with which the CWT trajectory is to be described
- the effect of the shape of the path of the CWT (square vs round implementation)
- the effect of the incomplete CWT twist-pitches
- the effect of the CWT twist-pitch length

The details of this results cannot be reported here. It suffices to say that in order to obtain results with a relative precision of 10^{-4} or better:

- the minimum number of points for the CSM single turn CWT trajectory is ~5000 (i.e. one every 2–3 mm)
- the shape of the CWT path plays a critical role, i.e. it needs to be a square path as in the real case
- incomplete CWT pitches have an important impact on the single turn CWT voltages (but are negligible at the level of 28 turns in a DP, see discussion later)

Table 3
Voltage in the CWT at 0.05 s into a fast discharge from 40 kA calculated in turns 1 & 294 for different CWT geometry implementations (CARIDDI A-method).

Turn	round shape (diameter 0.05 m)	Square shape (0.05 m side), sharp corner	Square shape (0.05 m side), round corner (r = 0.004 m)
Turn 1	−7.852983 V	−7.850542 V	−7.850294 V
Turn 294	−7.528833 V	−7.527541 V	−7.527470 V

- for the case of an integer number of pitches, the CWT twist pitch length has no impact provided the CWT path is described with a minimum number of points (this conclusion is limited to the 2D case).

Table 3 gives the CWT voltages for different turns of the CSM for different CWT trajectories (round, square, and square with rounded corners – see Fig. 5. All these calculations were performed with the minimum number of points specified (>5k/ turn) for the implementation of the path over which the vector potential is integrated. The path defined was for an integer number of pitches. In fact this calculation was performed only for one pitch (and multiplied with the number of pitches). As shown in the table the square shaped CWT (which is the one actually implemented in the CSM) captures a little less flux as it is placed a bit further from the conductor than the round shaped CWT, inscribed into the outer edge of the square jacket. Since there is hardly any effect of the rounded corners, the simpler CWT implementation with the sharp corners is used in the following.

4.2. Single turn voltages with the A-method (2D)

Table 4 summarizes the voltages obtained for the thick and thin conductor approximations. Again, as before for the vector potential (Table 2) there are significant differences for the different conductor implementations. The voltages averaged over the conductor (w. hole), column 3, are those that shall be used in the following discussion.

4.3. Comparison to ANSYS-Maxwell

As a cross-check a 2D model implementing the A-method was also developed with ANSYS-Maxwell (Fig. 6). The equivalent flux linked with each turn is computed as $\Phi_{eq}(t) = \frac{2\pi}{S}\int_S \rho \, A_\Phi(\rho, t) \, dS$ where ρ (m) is the distance of the considered sampling point from the z-axis, S (m^2) is the area of the turn's cross-section and the integral has been computed numerically through midpoint rule. This procedure is equivalent to decomposing each turn into 400 elements (blue grid, Fig. 6) and evaluating the flux linked with it as the weighted average of the fluxes linked with each element. The induced voltages are then obtained as the time-derivatives of the fluxes, which are computed via the central difference method.

Tables 5 and 6 show the comparison of the CARIDDI and ANSYS-Maxwell results, showing reasonable agreement.

5. Calculations of the voltage with the E-method

For taking into account the three-dimensional geometry of the superconductive system, we built a 3D model of the cable and we made the computation by means of the CARIDDI code. The code implements a discretized model of the following weak integral formulation in terms of the (unknown) current density

$$\mathbf{J} = -\sigma\left(\frac{\partial \mathbf{A}[\mathbf{J}(\mathbf{r},t)]}{\partial t} + \frac{\partial \mathbf{A}_S}{\partial t} + \nabla U\right)$$
$$\therefore \int_{V_c} \mathbf{W} \cdot \left(\frac{\partial \mathbf{A}[\mathbf{J}(\mathbf{r},t)]}{\partial t} + \frac{\partial \mathbf{A}_S}{\partial t} + \nabla U\right) d\tau + \int_{V_c} \mathbf{W} \cdot \sigma^{-1} \mathbf{J} d\tau = 0 \tag{5}$$

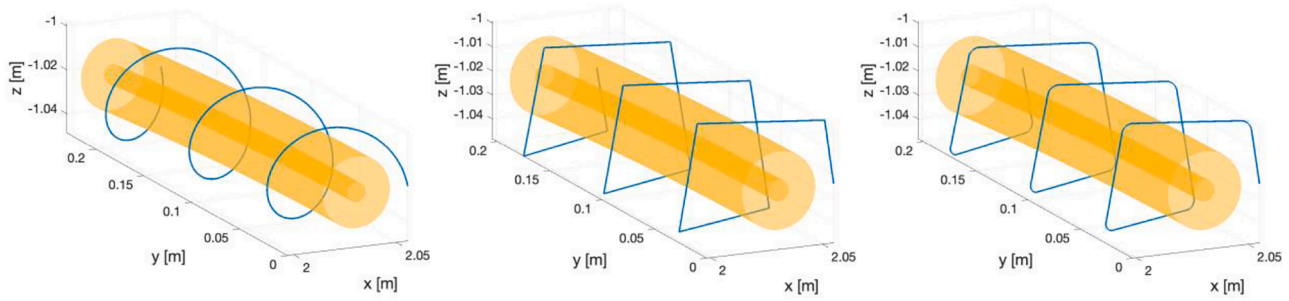

Fig. 5. Left – Round CWT path, center – square with sharp corners CWT path (as implemented in the simulation), right – square with round corners CWT path. The conductor is depicted in orange and for reference purposes only.

Table 4
Voltage in the turn at 0.05 s into a fast discharge from 40 kA calculated in turns 1 & 294 for different conductor geometry approximations (CARIDDI A-method).

Turn	Thick conductor (no hole) – from A in center	Thick conductor (no hole) – from average A	Thick conductor (w. hole) – from average A
1	−7.8686289 V	−7.864802 V	−7.8642911 V
294	−7.5376641 V	−7.53522 V	−7.5348404 V

$$\mathbf{J} \in \left\{ \mathbf{J} \in \mathbf{L}^2(V_c) : \nabla \cdot \mathbf{J} \in \mathbf{L}^2 \middle| \mathbf{J} \cdot \hat{\mathbf{n}} = 0 \text{ on } \partial V_c \backslash S_E,\ \mathbf{J} \cdot \hat{\mathbf{n}} = J_E \text{ on } S_E \right\} \tag{6}$$

Here, V_c is the conducting domain, **A**is the magnetic vector potential in V_c expressed in terms of **J** by means of the Biot-Savart law, $\mathbf{A}_S$is the magnetic vector potential due to the sources external to V_c, U is the electric scalar potential. S_E is the part of the boundary ∂V_c where the electrodes are located, J_E is the current density flowing through the electrodes

The solenoidality of **J**is imposed by assuming $\mathbf{J} = \nabla \times \mathbf{T}$ and a two component gage condition for **T**. The equation is discretized by using edge element shape functions $\mathbf{N}_k(\mathbf{r})$ for **T** and the tree-cotree gage condition [1,6]. Having expressed the current density as $\mathbf{J}(\mathbf{r},t) = \sum_{e \in \boldsymbol{E}} I_e(t) \nabla \times \mathbf{N}_e(\mathbf{r})$, where $\boldsymbol{E}$ is the set of DOFs (the Degrees Of Freedom corresponding to the active edges of the mesh) and applying the Galerkin method ($\mathbf{W}_k(\mathbf{r}) = \nabla \times \mathbf{N}_k(\mathbf{r}),\ k \in \boldsymbol{E}$), we obtain the following set of discretized equations

$$\begin{aligned} & L\frac{dI}{dt} + RI + H^T\Phi + \frac{dE^s}{dt} = 0 \\ & HI = \mathscr{I}_\Phi \end{aligned} \tag{7}$$

where I is the column vector made of the DoFs, Φ is the column vector made of the electrode potentials, $\mathscr{I}_\Phi$ is the column vector made of the corresponding electrode currents and

$$L_{ij} = \frac{\mu_0}{4\pi} \int_{V_c} \int_{V_c} \frac{\mathbf{w}_i(\mathbf{r}) \cdot \mathbf{w}_j(\mathbf{r}')}{|\mathbf{r} - \mathbf{r}'|} d\tau d\tau' \tag{8}$$

Table 5
Voltage in the CWT at 0.05 s into a fast discharge from 40 kA calculated in turns 1 & 294 with CARIDDI and ANSYS-Maxwell (A-method).

Turn	CARIDDI	ANSYS-Maxwell
Turn 1	−7.850542 V	−7.85108 V
Turn 294	−7.527541 V	−7.52779 V

Table 6
Voltage in the turn at 0.05 s into a fast discharge from 40 kA calculated in turns 1 & 294 with CARIDDI and ANSYS-Maxwell (A-method).

Turn	CARIDDI	ANSYS-Maxwell
1	−7.864291 V	−7.86420 V
294	−7.534840 V	−7.53492 V

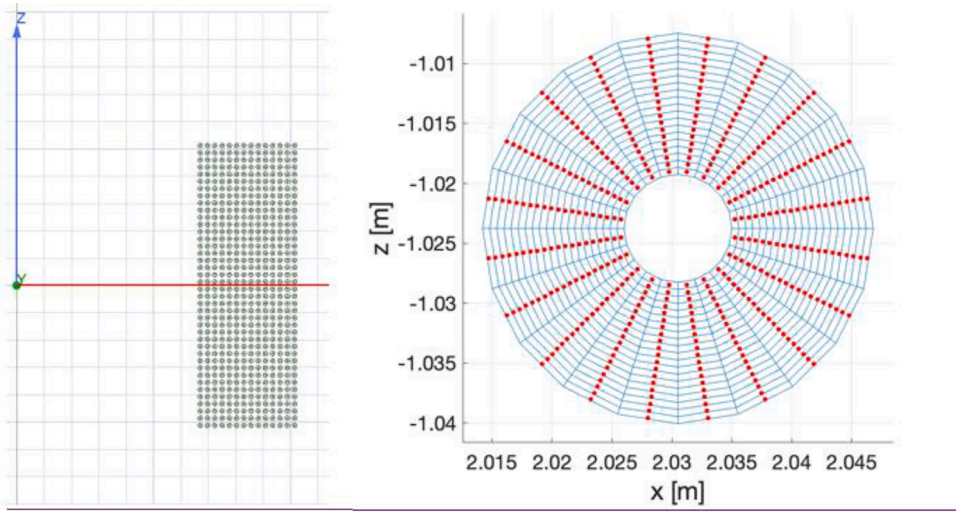

Fig. 6. Left – Axisymmetric representation of the CSM with 560 turns as implemented in Ansys Maxwell 2D. Right – Discretization of turn 1 implemented for the evaluation of the linked flux. The 400 red dots represent the sampling positions for the values of A_Φ (Vs/m).

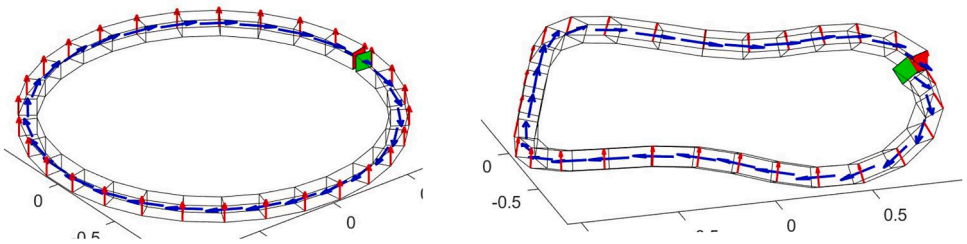

Fig. 7. Solenoidality of the current density automatically imposed with a very limited set of DOFs. The blue arrows represent the current density flowing in the conductor while the vertical red arrows represent the line integrals $I\int_{\ell_k}\mathbf{N}_k\cdot d\mathbf{l}_k$ describing the current I flowing into the coil. The two meshes show how the current density distribution conforms automatically to the distortion imposed by the helical pattern.

$$R_{ij} = \int_{V_c}\mathbf{w}_i(\mathbf{r})\cdot\sigma^{-1}\mathbf{w}_j(\mathbf{r})d\tau \tag{9}$$

$$H_{ij} = \int_{S_i}\int \mathbf{W}_j\cdot\hat{\mathbf{n}}_i dS \tag{10}$$

$$E_{s,i}(t) = \int_{V_c}\mathbf{W}_j\cdot\mathbf{A}_S(\mathbf{r},t)d\tau \tag{11}$$

In this context, it is important to note that the current flowing in a conductor and uniformly distributed can be modeled with only a line of hexahedral elements. As a matter of fact, for instance the current I_s across any facet S shared by two adjacent elements is given as (see Fig. 7):

$$I_s = \int_s\int \mathbf{J}\cdot\hat{\mathbf{n}}dS = \int_s\int \sum_{k\in\boldsymbol{E}} I_k(t)\nabla\times\mathbf{N}_k(\mathbf{r})\cdot\hat{\mathbf{n}}dS = \sum_{j\in\boldsymbol{E}_S} I_j\oint_{\partial s}\mathbf{N}_j\cdot d\mathbf{l}_j$$
$$= I_S\int_{\ell_e}\mathbf{N}_e\cdot d\mathbf{l}_e \tag{12}$$

In (12), $\boldsymbol{E}_S$ is the subset of $\boldsymbol{E}$ bounding S. In the example shown in Fig. 7, the only active edges are the edges drawn with red arrows. Therefore there is only one active edge bounding the cross section S. Notice that since all the red edges have the same value, the current flowing across any lateral surface is zero or because the edges bounding the lateral facets are not active or because their circulation is zero since all the red arrows have the same amplitude I_s. In the last equality in (12), we made use of the property of the edge elements giving $\int_{\ell_k}\mathbf{N}_k\cdot d\mathbf{l}_k = 1$ and $\int_{\ell_j}\mathbf{N}_k\cdot d\mathbf{l}_k = 0$

In our application, we can distinguish two different ways of simulating the cable fed by a set of electrodes with an impressed set of currents constant in time.

In the first way, the cable is supposed to be open at the ends so that the equations to be solved are

$$H^T\Phi = -\frac{dE^s}{dt} \tag{13}$$

Therefore, the sources of E^s include also the currents flowing into the cable. This case in a certain sense is still a 2D model since the field due to the sources is supposed to be axisymmetric. Actually there is a difference indeed, because if the electrodes are supposed to be equipotential it is evident that this can be obtained by the axisymmetric case only after averaging the values of the line integrals.

In the second way, the cable is fed by its own current so that the self feed is computed in its actual geometry. The model is therefore described by eqs (7), with $R = 0$.

Contrary to the A-method calculations (which are basically analytical), the E-method calculations, according to the previous section, are based on FE models. The advantage of this approach is that 3D effects

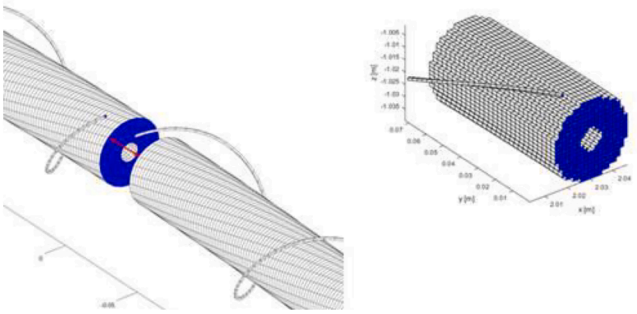

Fig. 8. Left: mesh of single turn thick conductor made of 35 electrodes (conductor twisted), showing the gap indicated by the double arrow (size of gap amplified for illustration purposes). Right: mesh of single turn thick conductor made of 292 electrodes (conductor untwisted).

can be simulated by injecting current into the conductor mesh (and building the conductor from twisted sub-cables). According to the experience gained in the A-method, the high precision (10^{-4} of better) requires a very accurate discretization. In particular this concerns the number of elements around the turn (>5000) and the sub-division of the conductor. Also the issues related to the time-derivation have to be considered as CARIDDI internally uses a back-ward scheme. This voltage has then to be corrected, averaging the voltage for the time point of interest and the next time instant (this is the central difference scheme implemented "through the back-door").

5.1. Single turn voltages with the E-method (2D)

The E-method 2D model is characterized by the fact that the meshed conductor does not carry current – it is only placed in the axisymmetric field produced by the coil, similarly as the CWT, to capture the flux. Examples of such conductor meshes are shown in Fig. 8. One consists of 292 petals arranged around a central hole. Assuming that as before for the CWT, 5000 elements along the turn provides sufficient accuracy, the mesh of each petal has 5000 elements along the turn, so a total of 1.5 M elements per turn. The conductor mesh has to cover the full turn (the gap, see Fig. 8, kept to <0.1 mm). Finally the axi-symmetric background turn behind the voltage sampling mesh has to be modelled with fine detail, i.e. implementing a 292 filament model to properly simulate the self-field. Note that there are different options for the multi-petals mesh

Table 7
Voltage in the turn at 0.05 s into a fast discharge from 40 kA calculated in turns 1 & 294 for different conductor meshes (CARIDDI, E-method).

	6 petals	48 petals	292 petals
Numb of elems	~30 k	~250 k	~1.5 M
Numb of nodes	~100 k	~1 M	~6 M
Turn 1	−7.86605 V	−7.86438 V	−7.86416 V
Turn 294	−7.53607 V	−7.53519 V	–

Table 8
CSM 1-turn voltage at 0.05 s into a fast discharge from 40 kA – difference between 2D and 3D model CARIDDI results.

Case	Turn 1 (V)	CWT 1 (V)	comp 1 (mV)	Turn 294 (V)	CWT 294 (V)	comp 294 (mV)	Type
straight conductor, no current	−7.86438	−7.8504	−13.99	−7.53519	−7.52750	−7.69	2D
twisted conductor, no current	−7.86438	−7.8504	−13.99	−7.53519	−7.52750	−7.69	2D
straight conductor, with current	−7.86467	−7.8504	**−14.28**	−7.53538	−7.52750	**−7.88**	2D
twisted conductor, with current	−7.86481	−7.85166	**−13.16**	−7.53548	−7.52835	**−7.13**	3D

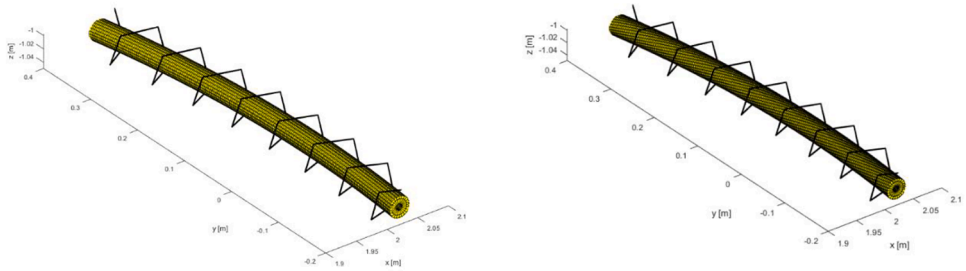

Fig. 9. Mesh of single turn thick conductor made of 48 petals and square path CWT. Left: conductor untwisted, Right: conductor twisted.

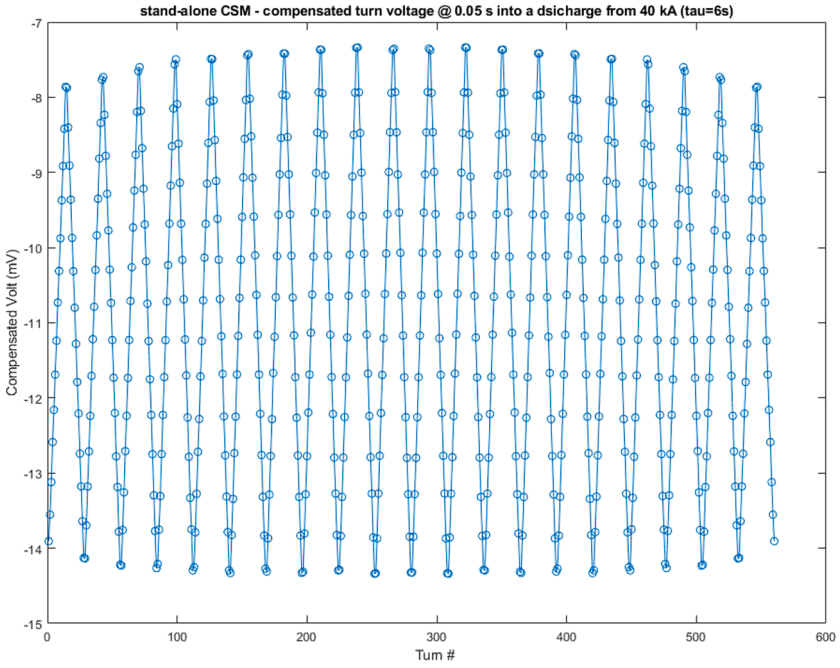

Fig. 10. Compensated voltage ΔV_{comp} for the turns of the CSM at 0.05 s after the start of the fast discharge from 40 kA calculated with the A-method (CARIDDI 2D model).

– the petals can be twisted or not, they can be insulated from each other or not, they can have any possible electrical resistivity. Generally it is best if the sub-conductors are insulated from each other, as this strongly reduces the number of DOFs in the mesh (to only 292 DOFs in the present example). Now, the 292 petal mesh in Fig. 8 is very large, requiring large computing resources even for one-turn calculations (high performance clusters or alike). A study was performed varying the degree of discretization of the mesh to find the minimum number of elements (Table 7). Comparing the data from Table 7 with those obtained with the A-method (Table 4), indicates that the required level of accuracy is already obtained with a 48 petal mesh. Note, however, that, as before with the A-method, single pitch models can also be implemented with the E-method, strongly reducing the model sizes (by a factor 10–100).

5.2. Single turn voltages with the E-method (3D)

The 3D model is characterized by the fact that the conductor does carry current – the respective turn is “switched off” from the axisymmetric background coil. Twisting (and insulating) the sub-cables in this model allows to simulate the 3D effect as discussed above. Note, however, that when the CWT and conductor have the same twist pitch, this effect does not appear in the compensated voltage. This was verified here. The results reported in Table 8 is for the case in which the CWT pitch is 76 mm (while the conductor pitch is ~0.45 m), as in the real CSM. In this case the 3D effect appears. Also in this calculation the CWT and turns are twisted in the same sense (anti-clock-wise), see the mesh plots in Fig. 9, as in the real CSM. When injecting the current into the mesh it is important that it flows in the same direction as for the axisymmetric back-ground coil.

Table 9
CSM DP voltage at 0.05 s into a fast discharge from 40 kA calculated with CARIDDI – difference between 2D and 3D model results.

DP location	DP #	ΔV (mV) CARIDDI-A-method 2D	ΔV (mV) CARIDDI-E-method 3D
bottom/ top	1	−308	−280
Middle	11	−305	−276

Note that preliminary experimental data from the CSM factory testing is ~400 mV for this case. A more in depth assessment of the experimental data is required, however, before concluding on a model to experiment comparison. The experimental profile of the current discharge, for example, was not a clean exponential function as assumed in these calculations. The impact of such (and other) specificities of the experiment still needs to be assessed. Also note that such voltages are considerably larger than the ~10 mV target, implying that the CWT scheme will not be sufficient for the ITER CS coil quench protection. Additional DP to DP signal compensation will be required.

The results shown in Table 8 indicate that the 3D effect reduces the compensated voltage by ~10%, i.e. ~1 mV (for opposite pitch sense between CWT and turn it would increase the compensated voltage by this amount). The 3D effect here is inferred from two calculations in which the current is injected into the mesh – one with non-twisted conductor (which is still a 2D case) and one with twisted petals, which generates the 3D effect (Fig. 8). The difference between these two cases is 1.12 mV for turn 1 and 0.65 mV for turn 294. At the level of a DP with 28 turns this gives a reduction of compensated voltage by ~30 mV.

6. Voltage of a complete double pancake

The smallest unit over which the voltage is recorded in the CSM is the Double Pancake (DP), which consists of 2 × 14 turns. Fig. 10 gives the results of a calculation of the compensated voltage, i.e. the difference of the inductive voltages picked up by the CWT and the turns as calculated with the A-method including all the model refinements discussed above in the context of single-turn models. This calculation is for the 2D limit. Table 9 gives a summary of the DP voltages calculated with all the models in this report. Note that in these calculations the turn- and layer-transitions are not modelled, but it was shown [5] that the impact is very small (note the self field “follows” the conductor along the transition). Also there inevitably is an incomplete pitch of the turn or the CWT (or both) at the end of the DP, which can give a non-negligible effect at the level of a single turn. But it was shown that this effect is divided by the number of turns in the DP (28) and thus becomes negligible [5].

7. Conclusions

Calculations of the voltages in the turns and CWT for the case of a stand-alone CS module during a fast discharge were performed with different methods, codes and models. Various issues related to the details of the model implementation were investigated and clarified. The conditions needed to achieve the required precision are discussed.

Declaration of Competing Interest

The authors declare that they have no known competing financial interests or personal relationships that could have appeared to influence the work reported in this paper.

Data availability

Data are published in the paper. Codess are not available

Acknowledgments

This work has received funding from the ITER Organization. The views and opinions expressed herein do not necessarily reflect those of the ITER Organization.

This work has been supported in part by Italian MUR under PRIN grant 20177BZMAH".

References

[1] R. Albanese, G. Rubinacci, Integral formulation for 3-D eddy \`current computation using edge elements", IEE Proc. 135 (1988) 457–462.
[2] ANSYS Maxwell https://www.ansys.com/products/electronics/ansys-maxwell 2022.
[3] P. Libeyre, et al., Detailed design of the ITER central solenoid, Fusion Eng. Des. 84 (2009).
[4] N. Martovetsky, et al., Normal-zone detection in tokamak superconducting magnets with co-wound voltage sensors, IEEE Trans. Magn. V32/4 (1997).
[5] G. Colombo, Laurea Thesis “Analisi Del Sistema Di Rilevamento Del Quench Del Solenoide Centrale Del Tokamak Di ITER, University of Bologna, 2022.
[6] R. Albanese, G. Rubinacci, Finite element methods for the solution of 3D Eddy current problems, Adv. Imaging El. Phys. 102 (1998) 1–86.